Experimental study on the bond behaviour between CFRP NSM strengthening system and concrete under fatigue loading

Javier Gómez[1*], Cristina Barris [1], Marta Baena [1], Lluís Torres [1] and Jose Sena-Cruz[2]

1. AMADE, Polytechnic School, University of Girona, 17003 Girona, Spain
2. ISISE/IB-S, University of Minho, Azurém,4800-058 Guimarães, Portugal

[*]Corresponding author email: javier.gomez@udg.edu

Abstract

Strengthening techniques based on the use of Carbon Fibre Reinforced Polymer (CFRP) materials have been used in bridges to extend their service life, since it has been proved their excellent performance under fatigue loading. Despite that, only few studies regarding the CFRP-concrete bond behaviour under fatigue loading can be found in the literature. Therefore, there is a further need of investigating how fatigue conditions can affect the behaviour of the bonded joints, since this affects not only serviceability aspects, such as crack width and spacing, but also the ultimate capacity of the strengthened elements.

This paper aims to contribute to the understanding of the bond behaviour of Near-Surface Mounted (NSM) CFRP-concrete specimens under fatigue loading. NSM CFRP-concrete specimens have been tested through direct pull-out tests under different fatigue loading conditions (20%-40%, 30%-50% and 40%-60% of the ultimate instantaneous load) at 5 Hz until 2.000.000 cycles. After the fatigue tests, specimens that did not fail under fatigue loading were tested monotonically until failure to study the residual bond response.

A significant increase of slip between the CFRP and the concrete at the loaded end was observed with the increasing number of cycles, being higher with the average load increase. Furthermore, a decrease on the stiffness of the cycle's loop and an increase of the residual slip were observed as the number of fatigue cycles increased. Finally, from the monotonic post-fatigue tests, a decrease on the load-slip stiffness was observed.

Keywords: Near-Surface Mounted (NSM), Carbon Fibre Reinforced Polymers (CFRP), Bond behaviour, Fatigue loading, Post-fatigue behaviour.

1. Introduction

During the last decades, the strengthening of concrete structures using Carbon Fibre Reinforced Polymers (CFRP) materials through the Near-Surface Mounted (NSM) methodology has been proved to be highly effective thanks to several advantages, namely, good anchorage capacity, high strengthening efficiency and protection against external agents, among others. In that sense, the bond behaviour of the FRP-concrete joint is of major importance to ensure an adequate transfer of shear stresses between materials. Some studies such as Sena-Cruz and Barros (2004), De Lorenzis and Teng (2007), Zhang et al. (2014), Bilotta et al. (2015) and Sharaky et al. (2013) extensively studied the instantaneous bond behaviour of NSM CFRP-concrete joints.

CFRP materials present an excellent fatigue behaviour (Alam et al. 2019, Song et al. 2019) and have been successfully used as strengthening systems to extend the service life of bridges (Alkhrdaji et al. 1999, Astorga et al. 2013). However, the behaviour of the NSM CFRP-concrete joint is affected by fatigue loading and further research needs to be carried out.

To simplify the study of fatigue bond behaviour between the strengthening system and the concrete element, direct shear pull-out tests have become the most used test configuration. Regarding the fatigue behaviour of CFRP Externally Bonded Reinforcements (EBR) in concrete elements, several experimental works can be found in the literature, e.g. Dai et al. 2005, Iwashita et al. 2007, Daud et al. 2015, Zhang 2016. These works reported that the fatigue load level at frequencies between 1-5 Hz has an important effect on the fatigue life of the bonded joint, being especially damaging for fatigue load levels beyond 50% of the instantaneous ultimate capacity, obtained at a lower speed of test. On the other hand, there are still several aspects, such as the residual ultimate capacity of the bonded joint after fatigue loading, where no agreement has been achieved yet. For that particular case, some works observed a decrease of the ultimate capacity (Daud et al. 2015), ranging between 13.3% and 27.5%, while others reported no variation (Zhang 2016) in comparison with the instantaneous ultimate load.

In recent years, some authors have studied the behaviour of NSM CFRP-concrete joint under fatigue loading, e.g. Dai et al. 2005; Yun et al. 2008; Fernandes et al. 2015; Chen and Cheng 2016 and Al-Saadi and Al-Mahaidi 2016. These works observed a general decrease of stiffness, but in terms of ultimate load carrying capacity after fatigue loading, different results and conclusions could be found: while Dai et al. (2005) (maximum stress levels of 51% and 73% P_u) and Fernandes et al. (2015) (stress levels of 23/52% and 26/59% P_u) observed a slight decrease, Chen and Cheng (2016) (stress level of 10/50% P_u) and Al-Saadi and Al-Mahaidi (2016) (stress levels of 10/60%, 10/67.5% and 10/70% P_u) did not observe any variation on the ultimate strength. Therefore, the fatigue bond behaviour of NSM CFRP-concrete joint needs further investigation to increase the knowledge of fatigue conditions on the strengthening system in terms of ultimate capacity of the structural element and serviceability aspects such as spacing and width of the cracks, deflections and the creep effect on the strengthening system.

This work aims to investigate the effect of the fatigue load level on the NSM CFRP-concrete bonded joint response. An experimental campaign consisting of six bond NSM CFRP-concrete direct shear pull-out specimens tested under different fatigue load levels at 5 Hz until 2,000,000 fatigue cycles was carried out. Furthermore, to study the residual bond behaviour of the bonded joints, a monotonic post-fatigue test were performed on specimens that withstood the fatigue cycles.

2. Experimental programme

The aim of this experimental work is to study the bond behaviour of NSM CFRP-concrete joints under fatigue loading. For this reason, six NSM CFRP-concrete specimens have been tested in a direct shear pull-out configuration under different load ranges (20%-40%, 30%-50% and 40%-60% of the ultimate load, P_u) at 5 Hz until 2,000,000 cycles. One of the fatigue tests under 30%-50% of P_u was carried out including unloading-loading stages to study how the monotonic loading stage was affected by fatigue cycles. Moreover, to study the effect of the groove width (or thickness of the adhesive layer), one specimen was prepared with 10 mm of the groove width, while in the rest of specimens the groove width was of 7.5 mm. The first value of groove width (10 mm) was set to satisfy the ACI 440.2R-08 requirement, i.e. the groove width must be 3 times the FRP strip thickness, while the second value

(7.5 mm) was adopted in agreement with *fib* bulletin 90 which establishes a minimum groove dimension of 1.5 or 2 times the FRP strip thickness.

The ultimate monotonic load, P_u was previously characterized in Gómez et al. (2020). In order to study the residual strength of the bonded joints after fatigue loading, specimens that withstood until the end of the test were tested monotonically until failure.

Table 1 lists the specimens tested in the experimental campaign with their respective groove width (t_g), maximum fatigue load (P_{max}) and level (S_{max}, defined as P_{max}/P_u), minimum fatigue load (P_{min}) and level (S_{min}, defined as P_{min}/P_u), fatigue ratio ($R = S_{min}/S_{max}$), number of cycles (N_c), ultimate load (P_u) and ultimate post-fatigue load ($P_{u,f}$). Each specimen was named as GW-S_{min}/S_{max} where W stands for the groove width in [mm]. For the case of G7.5-30/50, three specimens were tested, so the number of the specimen was added at the end of the name. One of them included unloading-loading stages (explained below) and was named as G7.5-30/50-U-L, where U-L stands for "Unloading-Loading".

Table 1. Direct pull-out tests under fatigue loading carried out in the experimental campaign.

Specimen	t_g [mm]	P_{max} [kN]	S_{max} [%]	P_{min} [kN]	S_{min} [%]	R	N_c	P_u [kN]	$P_{u,f}$ [kN]
G10-30/50	10	21.92	50	13.15	30	0.60	2,000,000	43.85	7.4**
G7.5-20/40	7.5	18.85	40	9.42	20	0.50	2,000,000	47.14	45.34
G7.5-30/50-1	7.5	23.57	50	14.14	30	0.60	2,000,000	47.14	23.8**
G7.5-30/50-2	7.5	23.57	50	14.14	30	0.60	2,000,000	47.14	46.9
G7.5-30/50-U-L	7.5	23.57	50	14.14	30	0.60	2,000,000	47.14	49.1
G7.5-40/60	7.5	28.28	60	18.85	40	0.67	1,646,763*	47.14	-

Note: * indicates premature failure in the gripping system during fatigue cycles and ** indicates premature failure in the gripping system during the monotonic post-fatigue test.

2.1. Material properties

To characterize the mechanical properties of the concrete, 150 mm × 300 mm cylindrical specimens were tested according to the ASTM C469 / C469M-10 and the UNE 12390-3 standards. An elastic modulus of 33.1 GPa (CoV 3.3%) and a compressive strength of 33.8 MPa (CoV 4.4%) were obtained from the characterization.

The CFRP strips used as a strengthening system were Sika Carbodur S with a cross-section of 3 mm × 10 mm. The mechanical properties were tested according to ISO 527-5:2009, obtaining a tensile strength and an elastic modulus of 3.2 GPa (CoV 2.1%) and 169.3 GPa (CoV 7.7%), respectively.

A bi-component epoxy resin Sikadur 30 was used as adhesive in the experimental campaign. Following the ISO 527-2:2012 standard, after 12 days of curing under 20 ºC and 55% RH, a tensile strength and an elastic modulus of 27.9 MPa (CoV 11.2%) and 10.7 GPa (CoV 4.4%) were obtained, respectively.

2.2. Experimental set-up

Fatigue loading tests were performed under a direct shear pull-out configuration as it is shown in Figure 1a. The concrete block was rigidly fixed with two steel reaction elements of 60 mm and 50 mm width

to avoid the vertical translation and rotation of the specimen. Figure 1b presents a schematic lateral view of the set-up and Figure 1c depicts the dimensions of the concrete block and the CFRP strips.

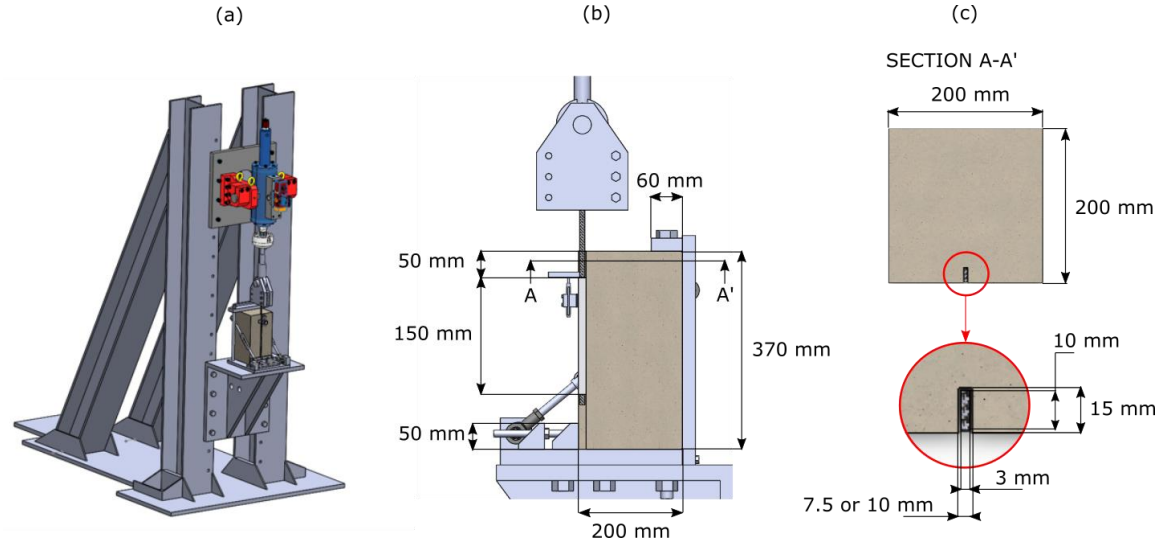

Figure 1: (a) Scheme of the fatigue set-up, (b) close up lateral view of the set-up and (c) detailed dimensions of the concrete block and the CFRP strip.

The concrete blocks dimensions used in the experimental campaign were 200 mm × 200 mm × 370 mm. From the top surface of the concrete block until the bonded length, 50 mm were left unbonded to avoid stress concentrations, then, a CFRP strip was bonded along 150 mm in all the specimens.

Fatigue tests were carried out in a servo-hydraulic testing machine (Servosis CH-9-100kN) with a stroke of 200 mm, a capacity of 100 kN and a maximum frequency of 50 Hz. An initial monotonic loading stage was performed under displacement control at a rate of 0.003 mm/s up to the average load of the fatigue cycles ($P_{avg} = (P_{max}+P_{min})/2$). Once the monotonic loading stage finished, the cyclic loading stage started at a frequency of 5 Hz and a load amplitude of (P_{max}-P_{min})/2. This frequency was selected because typical civil structures are loaded at frequencies ranging between 1 Hz and 5 Hz (Ferrier et al. 2005 and Zhang 2016). After 2,000,000 cycles, a monotonic instantaneous test was performed until failure under displacement control at a rate of 0.003 mm/s.

For the specimen G7.5-30/50-U-L, at every 200,000 fatigue cycles, an unloading-loading stage was performed consisting of an unloading stage where the load decreased monotonically until 2% of the P_u (to avoid possible compressions to the bonded joint, Carloni et al. 2012) followed by a loading stage until the P_{avg}. Once P_{avg} was achieved, fatigue cycles continued until the next U-L stage. In total, 10 U-L stages were carried out in the fatigue test.

The data acquisition was performed in two stages: (i) during the first two hours, all the measurements were recorded at a frequency of 50 Hz; (ii) after that, at every 5 minutes of testing, 10 seconds were recorded at 50 Hz.

The instrumentation consisted of a linear variable differential transducer (LVDT) placed at the loaded end to measure the relative displacement between the strengthening system and the concrete element, and a load cell to monitor the load applied to the specimen.

3. Analysis & discussion of results

All the specimens under fatigue load levels of 20%-40% and 30%-50% withstood 2,000,000 cycles without failure, but specimen under a fatigue load level of 40%-60% experimented a premature failure in the gripping system after 1,646,763 cycles.

From fatigue tests, the evolution of the slip at the loaded end (s) and the stiffness of the cycles (K_c, defined as the slope between the points of maximum and minimum load), were calculated.

Additionally, the stiffness of the monotonic loading stage (K_e) was studied through one fatigue test with ten unloading-loading stages (G7.5-30/50-U-L) to compare the degradation of the stiffness with cyclic loading. Furthermore, in this specimen the increase of the residual slip (s_0) with cycles was also measured. K_e was calculated as the slope between the final and initial points of the loading branch, while s_0 was taken as the slip at the end of the unloading stage.

Figure 2a represents how K_c was calculated from the load-slip curves obtained in the fatigue tests, and Figure 2b shows how K_c, K_e and the updated values of s_0 were measured from the fatigue test including unloading-loading stages.

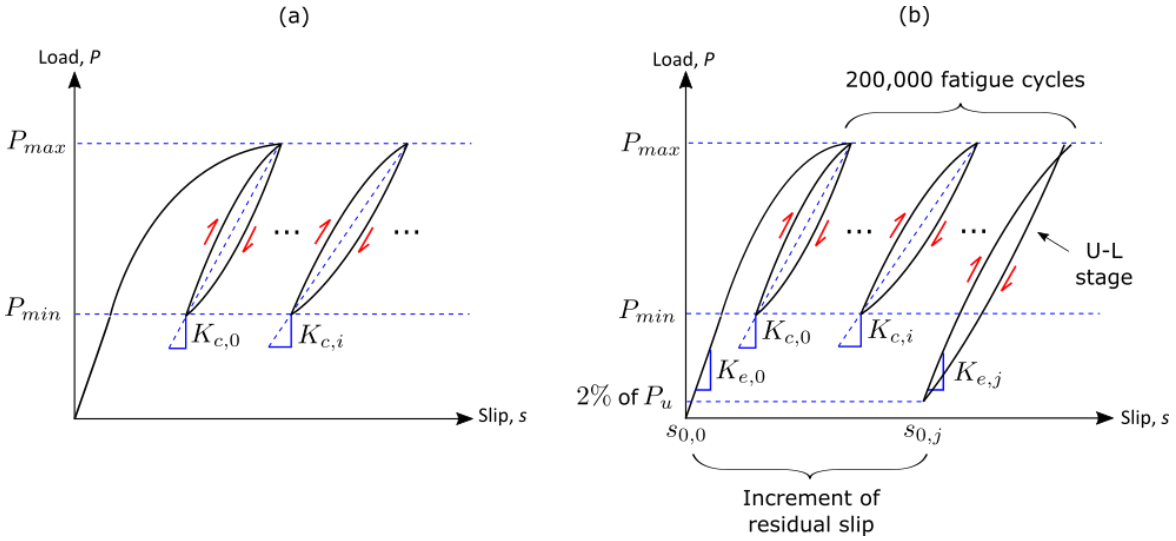

Figure 2: Studied parameters in (a) the fatigue tests and (b) the fatigue test including unloading-loading stages.

3.1. Evolution of the slip at the loaded end

In this section, the evolution of the loaded end slip with fatigue cycles is studied for each specimen configuration. For the test configuration G7.5-30/50, the average of the three cases tested is shown.

Figure 3 represents the evolution of slip with cycles for each specimen. Continuous lines represent the maximum slip (slip when P_{max} was achieved) and dashed lines represent the minimum slip (slip when P_{min} was achieved).

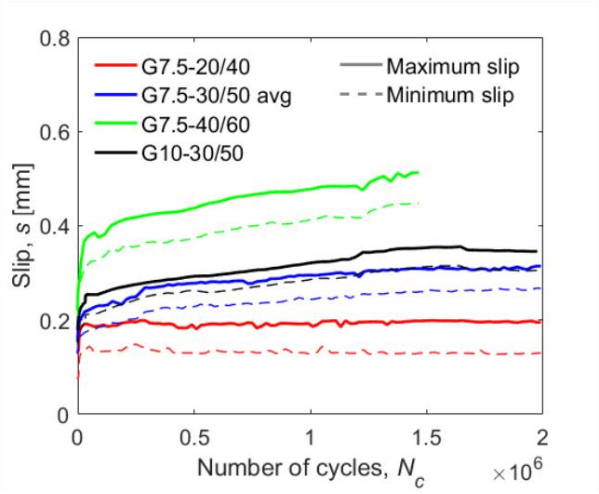

Figure 3: Evolution of maximum and minimum slips at the loaded end with cycles for each specimen.

During the initial cycles, all the specimens experimented a high non-linear increase of slip, and after some cycles the increase of slip became more linear.

As the fatigue load level increased, the slip at the loaded end increased as well, as expected. For fatigue load levels of 20/40 and 30/50, the slip at the loaded end tended to stabilize with fatigue cycles, while specimen under 40/60 experimented a continuous increase of slip with cycles.

Regarding the effect of the groove width, it can be seen that specimen G10-30/50, with a wider groove, yielded to slightly higher slips than specimens G7.5-30/50, indicating that the width of the adhesive layer is more affected by fatigue loading.

3.2. Degradation of the stiffness and the residual slip

The evolution of the stiffness of the cycle (K_c) for each specimen configuration and the stiffness of the unloading-loading stages (K_e) are presented in Figure 4a. To compare the degradation with respect to the corresponding initial value of stiffness at N_c = 0 cycles, Figure 4b presents the degradation of the stiffnesses normalized (k_c and k_e) obtained by using the value of the first cycle for each specimen, either K_c or K_e.

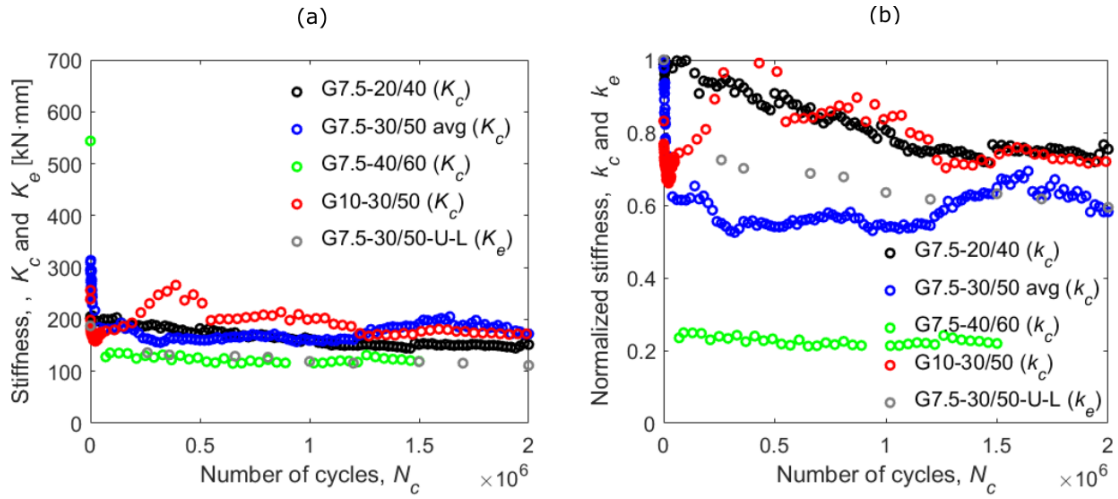

Figure 4: Decrease of (a) the stiffness and (b) normalized stiffness with cycles for each specimen.

Overall, a fast decrease of the stiffness during the initial cycles can be observed in all the specimen configurations, but around 20,000 cycles and beyond this point, a not significant reduction of stiffness was observed. Furthermore, it is observed that the specimen under the highest fatigue loading (40%/60% of P_u) obtained the highest decrease of K_c, indicating higher degree of damage in the bonded joint. On the other hand, similar degradation of K_c was observed in specimens under 20%/40% and 30%/50% of P_u during the fatigue test.

From Figure 4a it can be seen that in the specimen G7.5-30/50, a higher decrease of K_e in comparison with K_c was obtained. This is might be caused by the fact that the stiffness during the unloading-loading stage was not constant with load, and higher stiffnesses were achieved when the load was higher. Therefore, since K_e was calculated as the slope between the final and initial points of the loading stage, lower stiffnesses were obtained in comparison with K_c. However, as it can be seen in Figure 4b, k_c and k_e decreased similarly with cycles.

Furthermore, from the test G7.5-30/50-U-L, the increase of residual slip (s_0) was measured for every unloading-loading stage and is presented in Figure 5. A significant increase of s_0 was observed with cycles. This could be caused by the fact that the bonded joint experimented plastic deformations during fatigue loading, which could not be recovered during the unloading process (Zhang 2018).

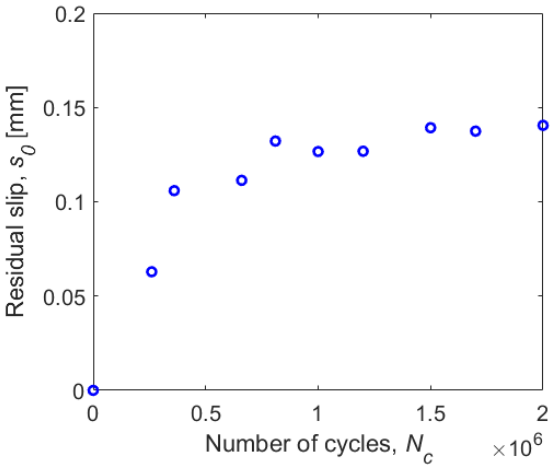

Figure 5: Increase of the residual slip (s_0) with unloading-loading stages (specimen G7.5-30/50-U-L).

3.3. Post-fatigue monotonic tests

To study the residual strength of the bonded joint, monotonic tests until failure were performed after two million cycles of fatigue loading. Figure 6 shows the load-slip curves obtained in the monotonic instantaneous tests (red curve), fatigue cycles (black curve) and the post-fatigue monotonic tests (blue curves) for specimens G7.5-20/40, G7.5-30/50-2 and G7.5-30/50-U-L. It should be noted that specimens G7.5-30/50-1 and G10-30/50 prematurely failed in the gripping system during the post-fatigue monotonic tests, and therefore, these tests are not shown.

From Figure 6, a residual slip was observed after fatigue loading, meaning that during fatigue loading, plastic deformations occurred in the bonded joint, and when the bonded joint was unloaded, it did not recover to the initial position.

Moreover, a reduction of the ascending stiffness at low loads could be observed in all the specimens after fatigue cycles. However, as the load in the post-fatigue monotonic test increased, a recovery of the stiffness could be seen, increasing the stiffness until reaching the monotonic instantaneous load-slip curve. This might be explained by the fact that during fatigue loading, only the activated length of the bonded joint was damaged, being the activated length lower than the bonded length, therefore, when the load in the monotonic post-fatigue tests surpassed the level of fatigue loading, the bonded length that was not damaged during fatigue loading was activated, and a recovery of stiffness could take place.

Finally, from the post-fatigue monotonic tests, it can be seen that the ultimate load of the bonded joint was similar to the values of P_u obtained in the monotonic characterization (see Table 1). On the other hand, a failure in the FRP-adhesive interface was obtained in all the specimens, while the failure mode in the monotonic instantaneous test was cohesive in the concrete. This change in terms of failure mode might be due to the damage caused by fatigue loading at the FRP-adhesive interface.

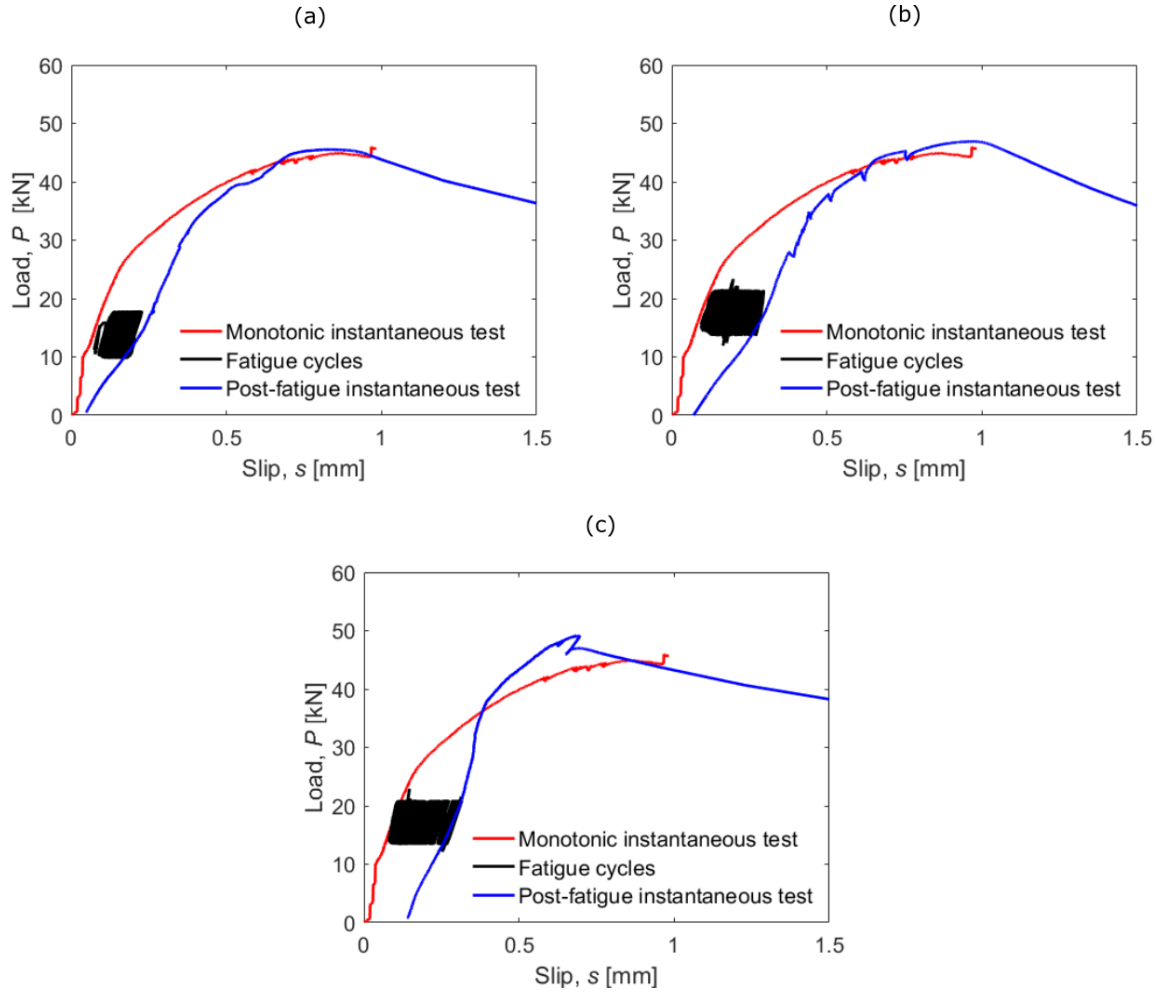

Figure 6: Load-slip curves obtained from the post-fatigue tests for cases (a) G7.5-20/40, (b) G7.5-30/50-2 and (c) G7.5-30/50-U-L.

4. Conclusions

This work presents an experimental study on the bond behaviour of NSM CFRP-concrete specimens under fatigue loading. Three fatigue load levels (20%/40%, 30%/50% and 40%/60% of P_u) and two groove widths (7.5 mm and 10 mm) were tested at 5 Hz for 2,000,000 fatigue cycles. Finally, monotonic tests after fatigue loading were performed in specimens that withstood fatigue cycles.

From the fatigue tests carried out in this study, the following conclusions could be stated:

- Higher increases of slip at the loaded end were obtained as the fatigue load level increased.
- A reduction on the joint stiffness was observed with fatigue cycles, being much more significant during the initial cycles.
- A similar decrease on the stiffness of the unloading-loading stages and the stiffness of the fatigue cycles with respect to their initial value, was observed.
- From the fatigue test with unloading and loading stages, an increase of residual slip and a decrease of the stiffness of the joint was observes as cycles increased.

From the monotonic post-fatigue tests performed in this work, it can be concluded that:

- A residual slip at the loaded end was measured at the end of the fatigue tests.
- An initial reduction of the stiffness of the post-fatigue load-slip curve followed by a recovery of the stiffness was observed in all the specimens.

- A failure mode in the FRP-adhesive interface was observed in all the specimens, probably caused by the degradation of the interface.
- The ultimate loads of the bonded joints were similar to values obtained in the monotonic instantaneous tests.

Acknowledgements

The authors acknowledge the support provided by the Spanish Government (MINECO), Project Ref. BIA2017-84975-C2-2-P. The first author acknowledges the University of Girona for conceding the IFUdG2018/28 and the MOB2019 grants. The authors also wish to acknowledge the support of SIKA Services AG for supplying the strips and the epoxy resin used in this study.

References

ACI 440.2R-08. (2008). Guide for the design and construction of externally bonded FRP systems for strengthening existing structures. ACI committee 440, . American Concrete Institute

Al-Saadi, NTK., Al-Mahaidi, R. (2016). Fatigue performance of NSM CFRP strips embedded in concrete using epoxy adhesive. Composite Structures, 154, 419–432.

Alam, P., Mamalis, D., Robert, C., Floreani, C., Ó Brádaigh, CM. (2019). The fatigue of carbon fibre reinforced plastics - A review. Composites Part B: Engineering, 166, 555–579.

Alkhrdaji, T., Nanni, A., Chen, G., Barker, M. (1999). UPGRADING THE TRANSPORTATION INFRASTRUCTURE: SOLID RC DECKS STRENGTHENED WITH FRP Tarek. Concrete International: Design and Construction, 21, 37–41.

ASTM C469 / C469M-10. (2010). Standard Test Method for Static Modulus of Elasticity and Poisson's Ratio of Concrete in Compression. ASTM International, Ed. West Conshohocken, PA

Astorga, A., Santa Maria, H., Lopez, M. (2013). Behavior of a concrete bridge cantilevered slab reinforced using NSM CFRP strips. Construction and Building Materials, 40, 461–472.

Bilotta, A., Ceroni, F., Barros, JAO., Costa, I., Palmieri, A., Szabó, ZK., Nigro, E., Matthys, S., Balazs, GL., Pecce, M. (2015). Bond of NSM FRP-Strengthened Concrete: Round Robin Test Initiative. Journal of Composites for Construction, 20, 04015026.

Carloni, C., Subramaniam, K V., Savoia, M., Mazzotti, C. (2012). Experimental determination of FRP-concrete cohesive interface properties under fatigue loading. Composite Structures, 94, 1288–1296.

Chen, C., Cheng, L. (2016). Fatigue Bond Characteristics and Degradation of Near-Surface Mounted CFRP Rods and Strips in Concrete. Journal of Composites for Construction, 20, 04015066.

Dai, JG., Saito, Y., Ueda, T., Sato, Y., Saito, Y. (2005). Static and Fatigue Bond Characteristics of Interfaces between CFRP Sheets and Frost Damage Experienced Concrete. Special Publication 230, 1515–1530.

Daud, RA., Cunningham, LS., Wang, YC. (2015). Static and fatigue behaviour of the bond interface between concrete and externally bonded CFRP in single shear. Engineering Structures, 97, 54–67.

De Lorenzis, L., Teng, JG. (2007). Near-surface mounted FRP reinforcement: An emerging technique for strengthening structures. Composites Part B: Engineering, 38, 119–143.

Fernandes, PMG., Silva, PM., Sena-Cruz, J. (2015). Bond and flexural behavior of concrete elements strengthened with NSM CFRP laminate strips under fatigue loading. Engineering Structures, 84, 350–361.

Ferrier, E., Bigaud, D., Hamelin, P., Bizindavyi, L., Neale, KW. (2005). Fatigue of CFRPs externally bonded to concrete. Materials and Structures/Materiaux et Constructions, 38, 39–46.

fib bulletin 90. (2019). Externally applied FRP reinforcement for concrete structures. International Federation for Structural Concrete

Gómez, J., Torres, L., Barris, C. (2020). Characterization and Simulation of the Bond Response of NSM FRP Reinforcement in Concrete. Materials, 13

ISO 527-2:2012. (2012). Determination of tensile properties-Part 2: Test conditions for moulding and extrusion plastics. International Organisation for Standardization (ISO), Ed. Geneva, Switzerland

ISO 527-5:2009. (2009). Determination of tensile properties - Part 5: Test conditions for unidirectional fibre-reinforced plastic composites. International Organisation for Standardization (ISO), . Geneva, Switzerland, Vol. 1

Iwashita, K., Wu, Z., Ishikawa, T., Hamaguchi, Y., Suzuki, T. (2007). Bonding and debonding behavior of FRP sheets under fatigue loading. Advanced Composite Materials: The Official Journal of the Japan Society of Composite Materials, 16, 31–44.

Sena-Cruz, J., Barros, JAO. (2004). Bond between Near-surface mounted carbon-fiber-reinforced polymer laminate strips and concrete. Journal of Composites for Construction, 8, 519–527.

Sharaky, IA., Torres, L., Baena, M., Miàs, C. (2013). An experimental study of different factors affecting the bond of NSM FRP bars in concrete. Composite Structures, 99, 350–365.

Song, S., Zang, H., Duan, N., Jiang, J. (2019). Experimental research and analysis on fatigue life of carbon fiber reinforced polymer (CFRP) tendons. Materials, 12

UNE 12390-3. (2003). Testing hardened concrete. Part 3: Compressive strength of test specimens. AENOR, Ed.AENOR, . AENOR, Madrid

Yun, Y., Wu, YF., Tang, WC. (2008). Performance of FRP bonding systems under fatigue loading. Engineering Structures, 30, 3129–3140.

Zhang, SS., Teng, JG., Yu, T. (2014). Bond Strength Model for CFRP Strips Near-Surface Mounted to Concrete. J. Compos. Constr., 18

Zhang, W. (2016). Experimental study on fatigue behaviour of CFRP plates externally bonded to concrete substrate. Structural Concrete, 17, 235–244.

Zhang, W. (2018). Prediction of the Bond–Slip Law Between Externally Bonded Concrete Substrates and CFRP Plates Under Fatigue Loading. International Journal of Civil Engineering, 16, 1085–1096.